telecom

MDPI

Article

An Alternative and Affordable DVB-T Feed for Small Gap Fillers

Ioannis Christakis [1,*], Spyridon Mitropoulos [2], Stylianos Katsoulis [1], Odysseas Tsakiridis [1] and Dimitrios Rimpas [1,*]

1 Department of Electrical and Electronics Engineering, University of West Attica, P. Ralli & Thivon 250, 12244 Egaleo, Greece; skatsoulis@uniwa.gr (S.K.); odytsak@uniwa.gr (O.T.)
2 Department of Surveying and Geoinformatics Engineering, University of West Attica, 28, Ag. Spyridonos Str., 12243 Egaleo, Greece; smitro@uniwa.gr
* Correspondence: jchr@uniwa.gr (I.C.); drimpas@uniwa.gr (D.R.)

Abstract

Digital television is an integral part of modern society, and the quality of the service its has exceeded all expectations. Television stations are divided into national and regional licensing categories, governed by the broadcasting regulations of each European Union member state. DVB-T gap fillers are used to provide and enhance the television signal in rural areas using satellite transport streams (TS) as feeds. However, for regional television stations—particularly in areas lacking network coverage—retransmitting their transport streams via standard digital terrestrial reception and rebroadcasting is often insufficient. This direct Re-transmission method frequently suffers from severe signal intermittency and broadcast interruptions. This paper presents the design, field deployment, and long-term evaluation (8760 h) of an ultra-low-cost, license-exempt DVB-over-IP gap filler architecture. The proposed system integrates Commercial-Off-The-Shelf (COTS) devices to convert a pristine DVB-T transport stream into an IP data stream, transmit it via a 5.64 GHz wireless bridge to bypass natural obstacles, and accurately reconstruct the digital TV signal at the remote gap filler. Empirical results demonstrate that the proposed IP stream method yields a 95.51% reduction in total annual downtime, elevating link availability from 86.26% to 99.38%. The system virtually eliminates environmental signal interruptions, with the only recorded downtime caused by a local power outage. Notably, this robust reliability is achieved at approximately 5% of the CEcapital expenditure (CapEx) required for conventional professional microwave backhaul solutions. Furthermore, the residual bandwidth of the wireless IP backbone provides a ready-made foundation for deploying future municipal network services, such as local Wi-Fi hotspots and LoRa-based Internet of Things (IoT) telemetry networks.

Keywords: DVB-T; signal; IP stream; simple gap filler; Re-transmission; TV

Check for updates

Academic Editors: Achilles Boursianis, Marica Amadeo and Sotirios K. Goudos

Received: 9 July 2026
Revised: 30 August 2026
Accepted: 16 September 2026
Published: 19 September 2026

Copyright: © 2026 by the authors. Licensee MDPI, Basel, Switzerland. This article is an open access article distributed under the terms and conditions of the Creative Commons Attribution (CC BY) license.

1. Introduction

Modern digital television relies on Coded Orthogonal Frequency Division Multiplexing (COFDM) signal modulation. Coverage areas are defined based on geography and are typically served by Single Frequency Networks (SFNs). In digital television (DVB-T), SFNs are described by application guides [1,2] as systems allowing gap-filling transmitters (using low-power synchronous transmission) to operate between master transmitter towers. The COFDM guard interval permits variable-length path echoes, simulating a scenario where multiple transmitters broadcast the same signal on a single frequency. DVB-T SFNs exploit this feature, though precise time and frequency synchronization remain a crucial requirement. Phase and frequency coordination between the transmitters relies on the adaptability of time-transfer systems, such as GPS (Global Positioning System) receivers (which are expected to produce PPS and 10 MHz signals) and other systems of a similar nature. The guard interval permits a timing budget, from which timing errors from the time-transfer mechanism can consume several microseconds [1]. In the worst-case situation, a GPS receiver may deliver a time within $+/-1$ µs, which is well within the system requirements of a DVB-T SFN in a typical configuration. Network transmission delays must be compensated to ensure synchronous broadcasting across all transmitters. In 'white areas'—regions lacking television coverage due to geomorphological electromagnetic shadowing (e.g., mountains)—deploying an unsynchronized gap filler offers a viable solution for digital TV radio coverage. Paper [3] presents the allotment zones and frequencies of use for SFN throughout the territory of Greece. Television programming is categorized into nationwide and regional stations. The nationwide stations transmit their programs throughout the territory of Greece, while the regional stations transmit their programs in the allotment zone where they are based. Main transmitters typically receive fiber-optic feeds from the DVB-T provider. Gap fillers acquire nationwide station feeds via satellite, whereas regional station feeds rely on direct off-air reception from the nearest main transmitter. Regional Re-transmission is particularly susceptible to weather variations, resulting in frequent signal dropouts during reception and rebroadcasting.

An important function of the gap filler is to suppress its own echo. In general, the manufacturers' technical specifications [4] state that the echo level at the gap filler input must not exceed the primary signal level by more than 12–15 dB. If the gap filler input signal increases disproportionately, the output signal drifts outside acceptable Modulation Error Ratio (MER) tolerances (<24 dB). Therefore, for reliable operation of the gap filler, sufficient signal isolation (not less than 80 dB [5]) must be provided between transmitting and receiving antennas.

The echo level limitation requirement also imposes a limitation on the output power of the gap filler [6]. In addition, there are other factors that limit the effectiveness of using a gap filler, such as:

- The output signal of the repeater, much like the echo, can vary with weather conditions;
- The phase difference between the repeater output signal and the echo can change due to antenna vibrations caused by wind;
- The signal reception conditions, especially from multiple points, may be disturbed due to secondary emissions reflected by local objects close to the receiving or transmitting antennas of the repeater.

In the literature, numerous studies have focused on predicting radio coverage and optimizing digital terrestrial transmission systems. The radio coverage performance of a Single Frequency Network (SFN) is optimized using simulated annealing (SA) [7]. This is achieved by using optimal values of internal static delays, antenna gains, and transmitter orientations. A corresponding optimization study [8] on a Digital Video Broadcasting–Second Generation Terrestrial (DVB-T2) network presents the use of a genetic algorithm (GA) as an optimization technique. These works aim to optimize the power and static time delays of transmitters in an SFN. Other papers [9,10] also focus on propagation prediction and optimization of SFNs used in various DTTB standards. In general, SFNs are costly both in design and deployment because of the need to avoid self-interference and ensure inter-transmitter synchronization. All the above-mentioned works refer to synchronized gap fillers. This case study addresses a geographic shadow area ('white area') completely lacking radio signal coverage. The novelty of this paper lies in the deployment of an affordable gap filler architecture that efficiently restores digital TV coverage in isolated areas where SFN synchronization is not required.

Inadequate radio frequency coverage is primarily caused by natural terrain obstacles (e.g., mountains, hills) that create electromagnetic shadowing. In areas of marginal coverage, challenges often arise from natural obstacles located at or below the line-of-sight altitude between the transmitter and the receiver. These obstacles obstruct the Fresnel zones [11] of the transmitted signal, causing vector smearing of the signal at the point of reception, while adverse weather conditions, such as high humidity, further degrade reception quality [12].

Interference caused by objects close to a radio beam's path can be analyzed using the concept of Fresnel zone clearance (Figure 1). It is imperative to maintain the first zone mostly free of obstacles in order to prevent radio reception interference. However, it is frequently acceptable to tolerate some occlusion of the Fresnel zones. Typically, 40% is the maximum obstruction that can be tolerated; still, 20% or less is advised [13]. The determination of the RF line of sight (RF LoS) is based on a straight line between the transmitting and receiving antennas, before creating any Fresnel zones. The Fresnel zone is then defined as the area around the RF LoS [14]. Each Fresnel zone's cross-sectional radius is largest at the RF LoS's midpoint decreases to a point at each vertex, behind the antennas.

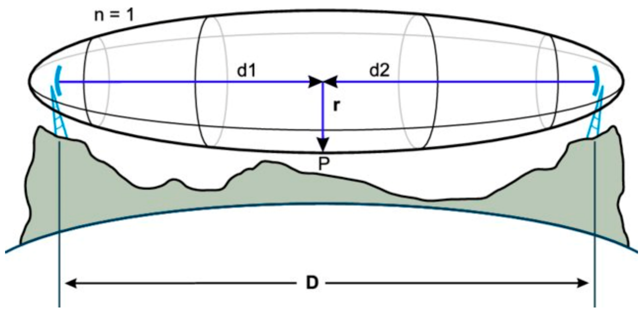

Figure 1. Fresnel zone [15]. D is the distance between the transmitter and the receiver; r is the radius of the first Fresnel zone (n = 1) at point P. Point P is on the middle of D, d_1 distance is equal to d_2 distance.

In general, the maximum clearance is given by the maximum radius of the first (n = 1) Fresnel zone. Using n = 1, d_1 = d_2 = D/2 and λ = c/f, where D is the distance (meters) between the two antennas, f is the frequency of the transmitted signal, and c ≈ 2.997 × 108 m/s is the speed of light in air.

The general formula for the radius of the first Fresnel zone is given in Equation (1).

$$F_1 = \sqrt{\frac{\lambda \cdot d_1 \cdot d_2}{d_1 + d_2}} \tag{1}$$

where λ is the wavelength (in meters), d_1, is the distance from the transmitter to the midpoint of the total distance of the pair (in meters), and d_2, is the distance from the midpoint of the total distance of the pair to the receiver (in meters).

In practical applications, the distances d_1 and d_2 are typically given in kilometers (km) rather than meters (m), and the operating frequency f is given in gigahertz (GHz) rather than hertz (Hz). The wavelength λ in meters is related to frequency f in Hz by Equation (2).

$$\lambda = \frac{c}{f} \tag{2}$$

where $c \approx 3 \times 10^8$ m/s is the speed of light in air. Expressing frequency f in GHz ($f \times 10^9$ Hz), Equation (3) yields the wavelength in meters:

$$\lambda(m) = \frac{c}{f \times 10^9} = \frac{3 \times 10^8}{f \times 10^9} = \frac{0.3}{f_{GHz}} \tag{3}$$

where λ is expressed in meters.

The general radius of the first Fresnel zone (F_1) in meters is defined by:

$$F_1(m) = \sqrt{\left(\frac{\lambda \cdot d'_1 \cdot d'_2}{d'_1 + d'_2}\right)} \quad (4)$$

where d'_1 and d'_2 are the distances in meters. Expressing distances in kilometers (d'_1 = $10^3 d_1$ and d'_2 = $10^3 d_2$) and substituting λ from Equation (4) into Equation (5) gives:

$$F_1(m) = \sqrt{\left(\frac{\frac{0.3}{f_{GHz}} \cdot (10^3 \cdot d_1) \cdot (10^3 \cdot d_2)}{10^3 \cdot (d_1 + d_2)}\right)} \quad (5)$$

Equation (5) leads directly to the standard practical formula for the first Fresnel zone radius shown in Equation (6):

$$F_1(m) = \sqrt{\left(\frac{300 \cdot (d_1 \cdot d_2)}{f_{GHz} \cdot (d_1 + d_2)}\right)} \quad (6)$$

At the midpoint of the link (d_1 = d_2 = D/2, where D is the total path distance in km), Equation (6) simplifies to Equation (7) [16]:

$$F_1 = \sqrt{\left(\frac{300 \cdot (D/2)^2}{f_{GHz} \cdot D}\right)} = \sqrt{\left(\frac{75 \cdot D}{f_{GHz}}\right)} \approx 8.66 \cdot \sqrt{\frac{D}{f_{GHz}}} \quad (7)$$

For the wireless link evaluated in this study operating at an exact frequency of f = 5.64 GHz over a total path distance D = 4 km, substituting these parameters into Equation (7) yields a maximum first Fresnel-zone radius at the midpoint (d_1 = d_2 = 2 km) as is shown in Equation (8):

$$F_1 = 8.66 \times \sqrt{\frac{4}{5.64}} \approx 7.29 \text{ m} \quad (8)$$

To ensure an unobstructed line-of-sight (LoS), at least 60% of the radius (0.6 × 7.29 m ≈ 4.37 m) must remain free from obstacles.

Understanding these Fresnel clearance requirements is critical when designing the 5 GHz microwave link utilized in this study, ensuring that the IP stream successfully bypasses the natural obstacles that obstruct standard UHF signals. In this paper, a cost-effective alternative solution for feeding a DVB-T gap filler, especially for re-transmission of television content from regional stations, is presented. The branded systems used to feed gap-filling transmitters, especially in SFNs, are costly to maintain. The case study presented in the above-mentioned paper concerns a shadowed area where the need for synchronization due to the SFN network is not essential.

Traditionally, continuous DVB-T signal coverage in mountainous or terrain-obstructed regions relies on broadcast gap fillers fed via two primary methods:

- Direct Off-Air Re-transmission (Transponders/Translators): Highly susceptible to severe fading, multipath interference, and low input MER (<19 dB), leading to frequent service outages.
- Professional Dedicated Backhaul: Carrier-grade microwave radio links (licensed 11–23 GHz bands) or satellite feeds utilizing professional DVB-over-IP gateways. While offering high availability, these systems incur substantial CEcapital expenditure (CapEx) and recurring spectrum licensing fees, making them economically unfeasible for local municipalities in underserved rural areas.

Rather than proposing a new physical layer transmission protocol, the novelty of this work lies in the integration, field deployment, and long-term empirical validation (8760 h) of an ultra-low-cost DVB-over-IP gap filler architecture operating over license-exempt spectrum. The specific contributions are framed across two distinct dimensions:

- Scientific and Methodological Contributions:
  - Empirical Reliability Proof over Unlicensed Spectrum: Demonstrates through a continuous 12-month empirical dataset (8760 logged hours) that baseband DVB-over-IP transport over the license-exempt 5.64 GHz ISM band can achieve carrier-grade availability (99.38%), delivering a 22.3 $\times$ Reliability Improvement Factor (RIF) over direct off-air transponding.
  - Statistical Validation Framework: Formally validates via paired hypothesis testing (t(11) = 11.42, $p < 0.001$, verified by Shapiro–Wilk and Wilcoxon signed-rank tests) that baseband Transport Stream reconstruction successfully mitigates severe end-to-end NLOS fading (67 km path) without relying on microsecond-level GPS SFN synchronization.
  - Minute-Level Outage Quantification: Establishes an exact one-minute temporal resolution framework (525,600 annual samples) based on the 10 dB MER Quasi-Error-Free (QEF) demodulation threshold of the DVB-T QPSK signal, accurately measuring outage reduction without artificial hourly overestimation.
- Practical Engineering and Economic Contributions:
  - Commercial System Cost Benchmark: Proves that integrating Commercial-Off-The-Shelf (COTS) 5.64 GHz hardware with a compact DVB-T regenerator (Terra ttx420) at €800–€1200 achieves broadcast-grade metrics (MER = 31.5 dB, latency < 7 ms, packet loss < 0.01%) comparable to commercial gap fillers costing €15,000–€25,000, representing a 95% CapEx reduction.
  - Zero Spectrum Fees and IoT Scalability: Eliminates recurring spectrum licensing costs (OpEx) while establishing a dual-purpose wireless IP backbone capable of supporting local telemetry and municipal IoT services (e.g., LoRa-based water monitoring [17]).

2. Materials and Methods

Field tests were conducted in the village of Pyrgos on Tinos Island, Greece, in the Cyclades archipelago. The village is surrounded by mountains that shield the area from electromagnetic radiation, preventing the reception of standard broadcast signals. Figure 2a shows both the area (village of Pyrgos, Tinos) where there is no broadcasting coverage and the digital television broadcasting centers on “Syros” and “Paros” Islands. Signal reception from the Paros broadcast center (67 km away) is marginal and suffers from constant interference, while signals from the Syros broadcast center are completely obstructed by local mountains (indicated by red ovals in Figure 2b). As shown in Figure 2b, Point A provides suitable reception from the ‘Syros’ broadcast center. This study utilizes two distinct reception nodes: Point A receives the DVB-T signal from Syros, while Point B receives the signal from the ‘Paros’ broadcasting center.

Figure 3 provides a panoramic view from an altitude of 372 m, illustrating the gap filler installation point, neighboring mountain peaks, and the geographically shadowed settlement.

In Figure 4, a panoramic view of the area (the image was captured from a mountain top at an altitude of 372 m) shows the gap filler installation point (Point B), the new reception and relay point (Point A), the broadcasting center in Paros (BC Paros), and the broadcasting center in Syros (BC Syros).

(**a**) (**b**)

Figure 2. The interest point for DVB-T coverage; (**a**) The village of Pyrgos on Tinos island and the official DVB-T broadcast centers of Paros and Syros; (**b**) Area of Pyrgos village with the natural obstacles (mountains) that surround it, as well as indicative high points (A & B) where a 5 GHz link can be established. The red circles mark the mountains located in the surrounding area.

Figure 3. Panoramic view of the geography of the area.

Figure 4. Panoramic view for DVB-T Broadcasting areas and shadow area (white area).

The following figures illustrate the elevation profile of the surface land between the above-described points and broadcasting centers (BC). The elevation profiles were captured using Google Earth Pro software (Version 7.3.7.1327 (64-bit)) [18]. Earth curvature is omitted from these profiles, as the relatively short transmission distances—particularly the 4 km 5 GHz radio link—render curvature effects negligible compared to local terrain obstacles. Figure 5 shows the elevation profile between the proposed reception Point A and the broadcasting center "Syros," and Figure 6 depicts the elevation profile between Point B, where the gap filler is installed, and the broadcasting center "Paros".

Figure 5. Elevation profile between Point A and broadcasting center "Syros". Each star mark represents the two points (A and B).

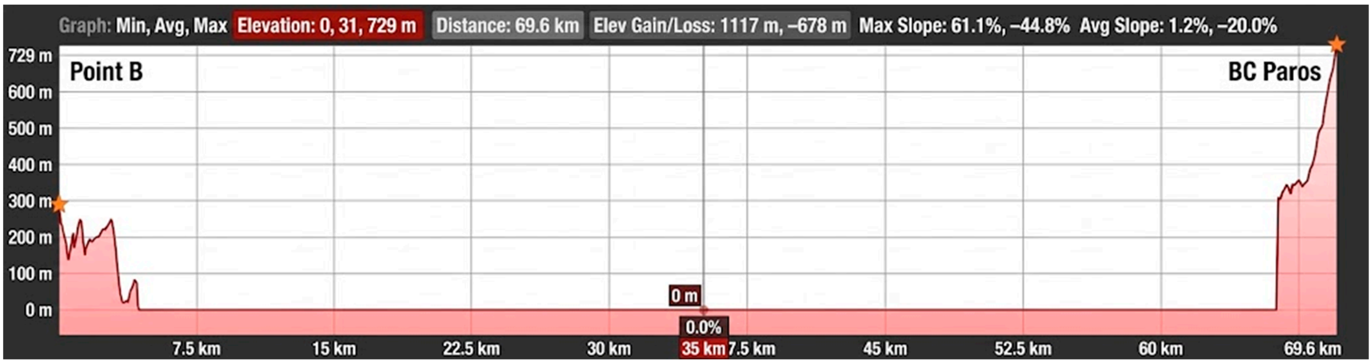

Figure 6. Elevation profile between Point B and broadcasting center "Paros". Each star mark represents the two points (A and B).

As illustrated in Figures 5 and 6, Figure 5 demonstrates an unobstructed LoS between the broadcasting center and the receiver, with both the broadcasting center and the receiver located at a high altitude. Figure 6 shows that while the Paros broadcasting center is elevated, the receiver (Point B) is positioned much lower, with a physical barrier obstructing the path immediately before the reception point. This terrain profile severely distorts the received television signal. Figure 7 depicts the elevation profile between Point A and Point B.

Figure 7. Elevation profile between Point A and Point B which are both represented by the star marks.

The placement of a DVB-T to IP stream unit at Point A provides the possibility of reliable reception without intermittency problems. The installation of a broadband wireless network link between Points A and B P(where Point B is the gap filler facility for television coverage in the area of interest) can provide the IP stream. As shown in Figure 2b, at point

B, the IP-stream-to-the-DVB-T device was used to regenerate the DVB-T transport stream (TS). The output of this device can drive the low-power TV transmitter (gap filler).

Hardware Architecture and Signal Processing Topology:

The hardware components utilized for DVB-T signal reception, regeneration, and re-transmission are illustrated in Figure 8. The installed components are as follows:

- A DVB-T to IP stream unit (Terra electronics (Kaunas, Lithuania)—sti410c [19]) as shown in Figure 8a, and a radio router in the 5 GHz frequency band (MikroTik (Riga, Latvia) RB-LHG-5GHz-24.5dBi [20]) as displayed in Figure 8b are installed at Point A;
- At Point B, an identical radio router (Figure 8b) and an IP-stream-to-the-DVB-T unit (Terra electronics—mi520 [21]) depicted in Figure 8c are installed

(**a**) (**b**) (**c**)

Figure 8. The materials were used for the reception, re-transmission, and regeneration of the DVB-T television signal; (**a**) Terra electronics—sti410c DVB-T to IP stream unit; (**b**) MikroTik RB-LHG-5GHz-24.5dBi radio router; (**c**) Terra electronics—mi520 IP stream to DVB-T unit.

To establish a rigorous baseline for evaluation, two distinct operational configurations were evaluated at the shadowed village re-transmission site (Point B):

- Legacy Direct Off-Air Configuration (Point B):
  Under the legacy configuration, the re-transmission node at Point B utilized a Terra ttx420 transmodulator to directly capture the off-air DVB-T broadcast from the regional broadcast center on Paros Island. In compliance with spectrum allocation regulations, the ttx420 demodulated the incoming RF signal, performed baseband regeneration, and transmodulated it onto a secondary frequency channel for local distribution. However, because Point B lacks a direct line-of-sight path and suffers from severe multipath environmental fading over the Paros path, this direct off-air link experienced frequent signal degradation (logging 106 discrete interruption events during the representative 1-month high-resolution observation period, 10 June–10 July 2024).
- Proposed IP Stream Backhaul Topology (Point A to Point B):
  To bypass the unstable off-air path, an alternative reception site was established at Point A, located 4 km away from Point B and possessing an unobstructed line-of-sight path to the primary broadcast center on Syros Island. The proposed architecture operates through the following processing chain:

- Primary Capture Node (Point A): A Terra sti410c streamer demodulates the robust DVB-T signal received from Syros and encapsulates the Transport Stream into an IP multicast stream.
- Wireless IP Transport: The IP stream is relayed across the 4 km link between Point A and Point B via a 5.64 GHz MikroTik wireless IP bridge.
- Local Regenerator and Transmitter Node (Point B): At Point B, a Terra mi520 IP-to-DVB-T gateway receives the IP stream, de-encapsulates the payload, and reconstructs a high-MER DVB-T RF output channel for local distribution to the village.

The CEcapital expenditure for the 5 GHz radio link hardware is under €200. This low cost makes the solution highly accessible for small-scale gap filler deployments, especially compared with conventional microwave links and professional regeneration units. The implementation topology was established in two phases, as distinct installations are required for each system operation point, Point A and Point B, respectively. In particular, Figure 9a shows the interconnection topology of the components used at point A; more specifically, the systems include an antenna in the UHF (Ultra High Frequency) frequency band, a DVB-T-to-IP stream unit (Terra electronics—sti410c), and a wireless router antenna (MikroTik RB-LHG-5GHz-24.5dBi), which are housed in a metal box for protection against weather conditions. Figure 9b illustrates the interconnection topology of the components used at Point B, where the following components were utilized: A wireless router antenna (MikroTik RB-LHG-5GHz-24.5dBi) and an IP- stream-to-DVB-T (Terra electronics—mi520) unit, which are housed in the facilities of the district's TV transponder (gap filler).

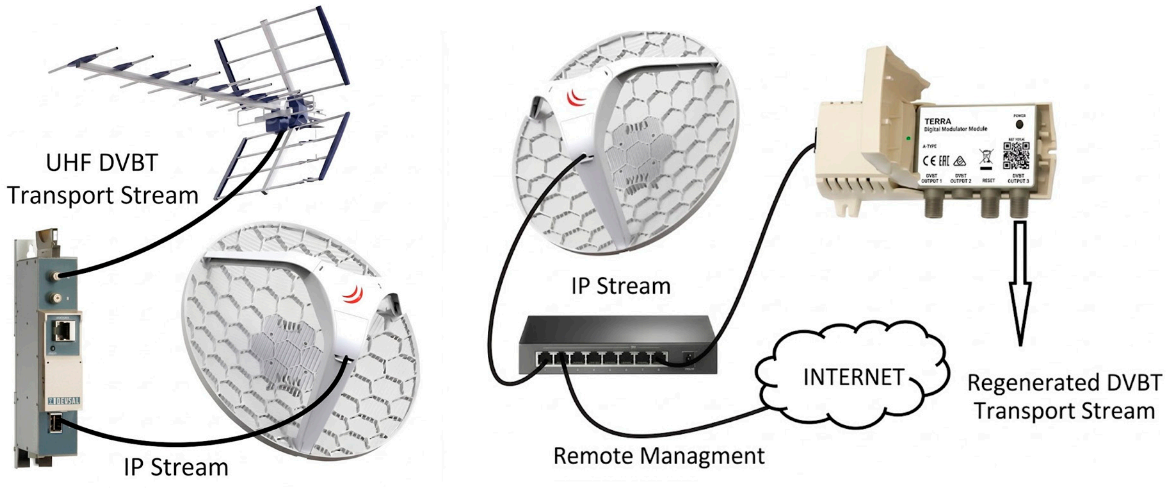

(**a**) (**b**)

Figure 9. The topology of the implementation of Points A and B; (**a**) Point A installation materials, DVB-T reception, conversion to IP stream, and transmission of the IP stream via RF link to Point B; (**b**) Point B installation materials, IP stream reception via RF link, conversion (reconstruction) to DVB-T, and feed to transmitter.

The operation of the system requires all devices to be on the same subnet. The sti410c device receives the TV signal via the antenna. For reception, it supports QPSK, QAM16, and QAM64 (Quadrature Amplitude Modulation) with a channel bandwidth of 7/8 MHz, while for IP output it supports bitrates up to 100 Mbps and UDP (User Datagram Protocol) and RTP (Real-Time Protocol) transmission protocols. The same device decodes the transport stream into separate streams and assigns each stream to a different IP address and port. In this way, the network interface of the device provides a different IP address to each stream. The mi520 device, configured to receive stream data from a specific IP address and port, can substitute up to four streams, which are then multiplexed, to create a transport stream that is modulated at a specific frequency. The supported modulation schemes include QPSK (Quadrature Phase Shift Keying), 16-QAM, and 64-QAM, accommodating 7/8 MHz channel bandwidths, guard intervals of 1/4, 1/8, 1/16, and 1/32, and code rates of 1/2, 2/3, 3/4, 5/6, and 7/8. Regarding network flow, it supports a bit rate up to 80 Mbps and supports the UDP, RTP, and RTSP protocols; UDP at the transport layer; video coding for H.264 and H.265 samples; and AAC audio coding. The network connection between the two devices is achieved through the radio link (Wi-Fi—5 GHz). The output of this device is routed to the input of the gap filler.

Specifically, MikroTik RB-LHG-5GHz devices support the wireless transmission protocol 802.11n (20/40 MHz XX) [22], which was selected for operation, while the transmission power was set at 3 dBm. The 5 GHz radio link between the two sites maintains a signal-to-noise ratio (SNR) of approximately 55 dB, while the wireless Client Connection Quality (CCQ) and Tx/Rx CCQ range from 85% to 95%. The percentage value of CCQ [23] shows how effectively the frequency bandwidth is used with respect to the maximum possible bandwidth of the data rate. The management of all the devices described above, both DVB-T to IP and IP to DVB-T devices, as well as wireless networking equipment, is possible through a website interface. Connecting this infrastructure to the internet enables comprehensive remote management, telemetry monitoring, and holistic system supervision. Figure 10 shows the point of installation of the gap filler and, in particular:

1. Figure 10a displays the facilities of both the building and the antenna pylon;
2. Figure 10b illustrates the building where the gap filler is located;
3. Figure 10c depicts the devices used for the implementation of the gap filler.

The installation is located at the geographical position (37.654303, 25.022047) at an altitude of 264 m above sea level, while the height of the antenna pylon is 23 m.

(**a**) (**b**) (**c**)

Figure 10. The gap filler installation point; (**a**) The facilities of the gap filler (building and pillar of antennas); (**b**) The building where the gap filler is installed (Point B); (**c**) Gap filler device installation.

Outage Measurement Methodology and Modulation Thresholds:

To accurately quantify link availability without overestimating downtime, outage statistics were collected at a high-resolution 1 min sampling interval (525,600 logging events/year). The transmission employed QPSK modulation, which requires a minimum Modulation Error Ratio threshold of MER $\geq$ 10 dB to maintain Quasi-Error-Free (QEF) Transport Stream decoding.

An outage state ($S_i = 1$) was flagged for any 1 min interval in which the QPSK signal dropped below 10 dB MER or suffered TS synchronization loss; otherwise, the interval was recorded as operational ($S_i = 0$). Cumulative annual downtime (D_{total}, in hours) was calculated via exact minute summation $D_{total} = \frac{1}{60}\sum S_i$. This precise fractional formulation prevents artificial hourly overestimation and provides an accurate, minute-level assessment of network availability.

3. Results and Discussion

To ensure reproducibility and rigorous data collection, the experimental protocol was structured around standardized measurement hardware, strict signal loss criteria, and multi-tier evaluation timeframes:

1. Hardware, Software, and Antenna Characteristics

- RF Field Instruments: DVB-T signal parameters (RF power level, MER, cBER, and vBER) were measured using a calibrated Rohde and Schwarz field analyzer connected to the RF monitoring ports of the Terra ttx420 regenerators.
- IP Network Monitoring: Packet loss, latency, and jitter on the 5.64 GHz microwave link were continuously monitored using MikroTik SNMP Network Monitor integrated with Terra SNMP Agent software for deep packet inspection.
- Antenna Specifications:
    - DVB-T Reception (Points A and B): High-gain 18-element Yagi-Uda directional antennas (14.5 dBi gain, horizontal polarization, installed 2 m above ground level).
    - 5 GHz IP Bridge: Parabolic dish antennas (24.5 dBi gain, 7° 3 dB beamwidth).
- Monitored Multiplex and Frequencies: The monitored DVB-T multiplex operated on UHF Channel 44 (658 MHz, 8 MHz bandwidth, QPSK, code rate 3/4, guard interval 1/4). The point-to-point IP transport link operated at an exact center frequency of f = 5.64 GHz with a 20/40 MHz CE channel bandwidth.
- Sampling Interval: Raw RF and IP parameters were sampled at one-second intervals and aggregated into one-minute average log records.
- Operational Thresholds and Modulation Parameters: Based on the ETSI EN 300 744 standard for QPSK DVB-T reception, the Quasi-Error-Free (QEF) demodulation threshold (corresponding to a pre-Viterbi BER $\leq 2 \times 10^{-4}$) is physically bounded at MER = 10 dB. To ensure robust link monitoring and evaluate fading margins well above the physical breakdown limit, operational quality benchmarks were established at MER = 18 dB (minimum acceptable broadcast delivery) and MER $\geq$ 21 dB (optimal high-margin reception). The RF receiver sensitivity threshold was set to −52 dBm.
- High-Resolution Outage Logging Methodology: A physical signal loss event was strictly defined as any state in which the received signal dropped below the QEF limit (MER < 10 dB) or Transport Stream (TS) synchronization loss occurred. Telemetry data were continuously recorded at a high-resolution one-minute sampling interval (525,600 annual samples). To eliminate artificial hourly block overestimation, total cumulative annual downtime was calculated directly from the exact non-operational one-minute intervals.

The evaluation and the analysis of the measurements were conducted across three interconnected temporal scales:

- Five-Day Period: High-resolution stress testing (one-second logging resolution) focused on micro-scale packet transport dynamics (latency, jitter, and burst packet loss).
- Month Period: A focused worst-case monthly case study (720 h) evaluating link performance during peak ducting and multipath fading conditions (December 2024).
- Year Period: Macro-scale long-term reliability monitoring (8760 h, June 2024–May 2025) providing annual availability statistics and seasonal variation trends.

Empirical results validate the core system design, demonstrating improved signal delivery to the gap filler by leveraging Fresnel zone clearance relative to the transmission frequency. Under legacy operations, the gap filler was fed by a terrestrial TV signal at 658 MHz. The distance between the transmission point ("Paros") and the reception point (Point B) is 67 km. According to Fresnel theory (formula), the radius at the maximum point is 88 m. Given that the heights of the antennas are more than 250 m (height of the land surface and antenna mast) and the morphology of the terrain at the reception point, it is observed that the lower lateral Fresnel zone is continuously influenced by the geomorphology of the area at a distance of about 12 km. This obstruction causes severe multipath fading and reception intermittency, heavily exacerbated by atmospheric variations (e.g., humidity and temperature fluctuations), leading to poor re-transmission quality. The proposed architecture resolves this by relocating the primary reception site to Point A, which secures an unobstructed 28 km LoS path to the "Syros" transmitter at a height of 250 m. The signal is then relayed to Point B via a 5 GHz wireless bridge. At this higher frequency and shorter 4 km distance, the maximum Fresnel radius shrinks to just 7.4 m, easily clearing local obstacles.

This topology can be applied to cover TV content in isolated broadcasting areas that are not part of an SFN. Because the area lacks existing DVB-T radio coverage, GPS-based synchronization of the digital TV signal at the transmitter is unnecessary. The RF link in the 5 GHz frequency band was made using the 802.11n protocol with a transmission power of 3 dBm. The link employed a 2 × 2 MIMO configuration and achieved a measured symmetric data throughput of approximately 160 Mbps under the experimental conditions. Because the TV multiplexer requires 10 to 20 Mbps, the 160 Mbps capacity of the 5 GHz RF link provides substantial overhead to support supplementary services such as remote management of this layout and complementary devices, including a Lora gateway or wireless network to create a spatial coverage area for supporting Internet of Things (IoT) devices which are used in this area [24–27]. Figure 11 shows the signal status at Point A (receiver of "Syros", distance 28 km) in Figure 11a and at the gap filler installation Point B (receiver of "Paros", distance 67 km) in Figure 11b.

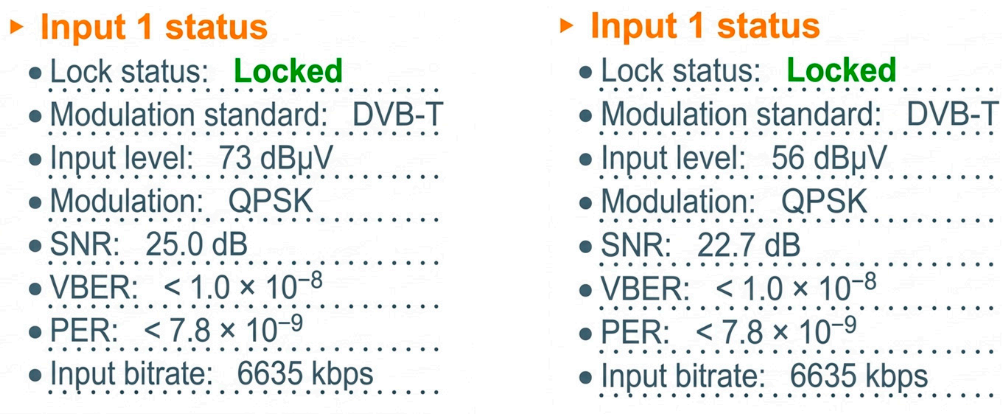

(**a**) (**b**)

Figure 11. Signal status of Point A and Point B; (**a**) Signal status at Point A—receiving "Syros"; (**b**) Signal status at Point B—receiving "Paros".

As shown in Figure 11, signal reception at Point A is markedly superior, exhibiting an input level of 73 dBμV compared with 56 dBμV at Point B. Additionally, the SNR is higher at Point A (25.0 dB) than at Point B (22.7 dB). Consequently, Point A provides a vastly superior reception feed for the regional transport stream.

End-to-End System Evaluation and Coverage Area Verification

To clearly isolate the source of improvement and address the end-to-end performance of the proposed architecture, synchronous field measurements were conducted across the complete signal path:

- Direct Off-Air Reception at Point B (Legacy link): Located 67 km from the main broadcast station with significant terrain diffraction near the receiver. The received RF power level was −79.5 dBm with a Modulation Error Ratio (MER) of 17.2 dB, dropping below the minimum acceptable broadcast delivery benchmark for QPSK (MER < 18 dB). This resulted in high post-Viterbi Bit Error Rates (vBER = 4.2 × 10^{-4}), uncorrectable Transport Stream (TS) packet loss (8.4%), and an average monthly outage duration exceeding 100 h.

- Primary Feeder Reception at Point A: Positioned at a high-elevation site 28 km from the transmitter with unobstructed line-of-sight (LoS). Point A achieved an RF level of −56.2 dBm, an MER of 32.8 dB, and zero packet loss (vBER < 10^{-8}).
- IP Transport link (Point A to Point B): The pristine TS received at Point A was encapsulated into IP packets and transmitted over the 5.64 GHz wireless bridge to Point B. The IP link exhibited highly stable performance, with a low average latency of 6.2 ms, jitter below 1.1 ms, and packet loss under 0.01%.
- Re-transmission and Final Coverage Area: At Point B, the compact DVB-T regenerator (Terra electronics mi520) processed the incoming IP stream and re-transmitted the RF signal into the shadowed local valley. In-field measurements in the target coverage area (1.5 km from the gap filler) confirmed full service restoration: an RF power level of −58.4 dBm, MER of 31.5 dB, 0% TS packet loss, and an annual link availability exceeding 99.3%.

Technical Limitations and Operational Constraints

While the proposed COTS-based DVB-over-IP architecture provides an exceptionally high cost-to-performance ratio, its technical boundaries must be explicitly emphasized:

- SFN Synchronization Exclusion: The intrinsic network jitter (<1.2 ms) and packet encapsulation delay (~6.2 ms) introduced by the COTS IP bridge prevent the system from achieving the microsecond-level GPS timing precision required for Single Frequency Network (SFN) topologies. Therefore, this system is strictly restricted to Multi-Frequency Networks (MFN) or localized gap fillers utilizing independent local RF channel conversions, where self-interference from co-channel transmitters is geographically shielded by terrain contours.
- Mandatory LoS Backhaul Link: Although the architecture successfully restores coverage across a 67 km terrain-obstructed path, it remains critically dependent on securing a completely clear primary Line-of-Sight (LoS) over the 28 km backhaul segment. Maintaining first Fresnel zone clearance across this 28 km link is mandatory to prevent primary link degradation.
- 5 GHz ISM Band Throughput and Interference Ceilings: Operating within the license-exempt 5 GHz ISM band eliminates spectrum fees but subjects the link to potential co-channel interference in crowded RF environments and imposes maximum throughput limits compared to professional licensed microwave backhauls (11–23 GHz). This trade-off renders the solution optimal for standard multi-program Transport Streams (MPTS) rather than high-density ultra-wideband backhaul.

Testing for this experiment was conducted over a full year, from the summer of 2024 through the summer of 2025. The data analysis was broken down by season to highlight the impact of weather and barometric conditions on the radio signal. Measurements recorded the signal strength received at the two aforementioned television signal reception points, A and B, from both the Syros broadcast center and the "Paros" broadcast center. Figure 12 illustrates the monthly received signal strength (in dBμV) at reception Points A and B from their respective broadcast centers.

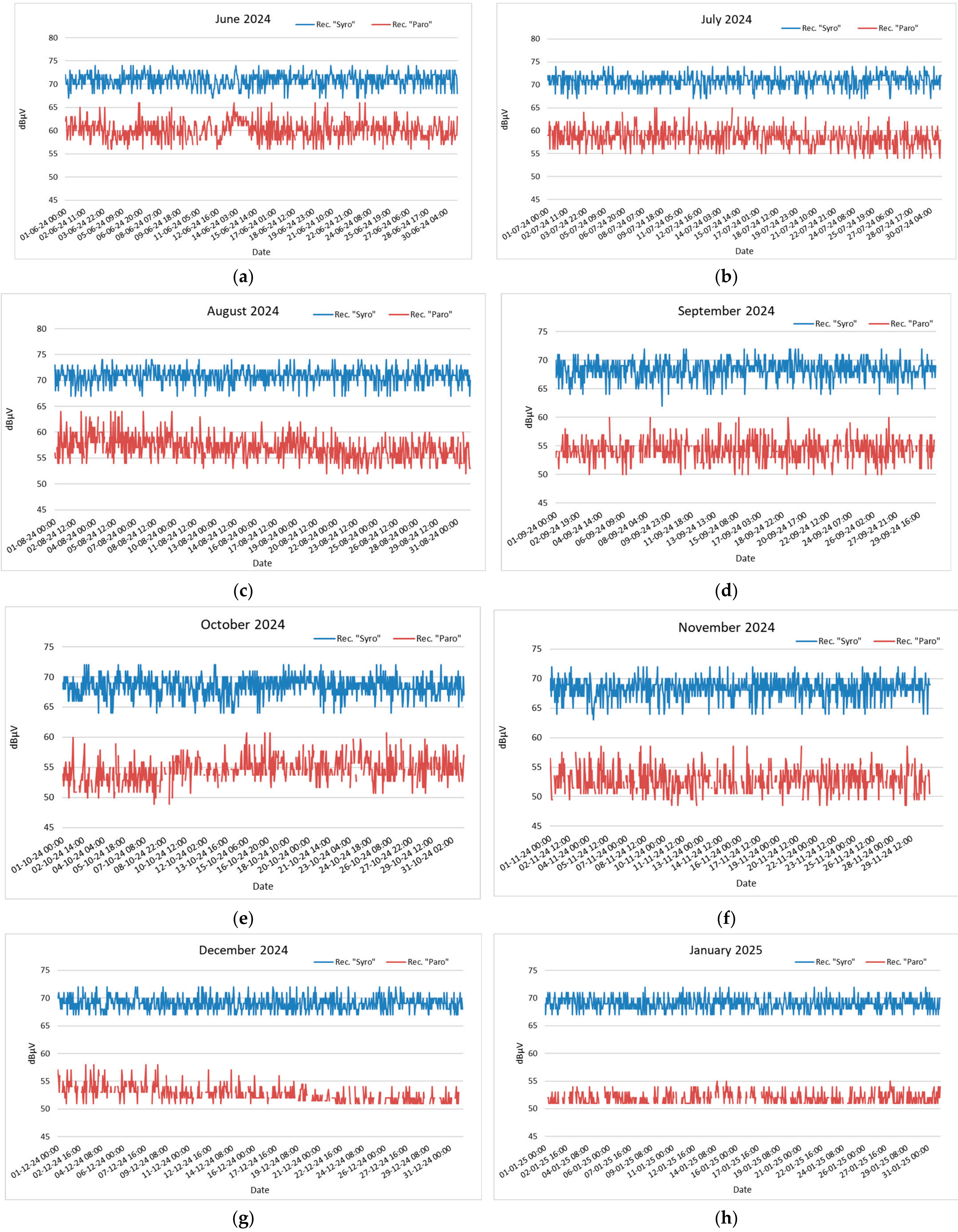

Figure 12. *Cont.*

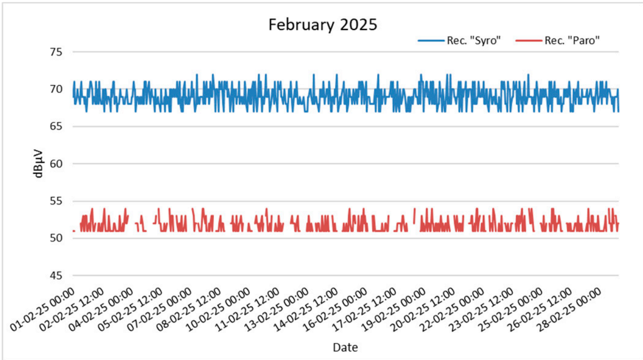

(**i**)

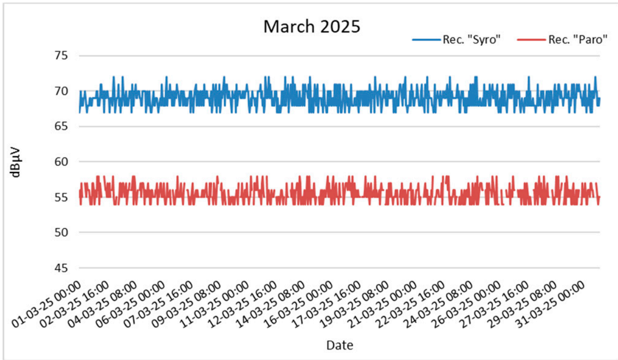

(**j**)

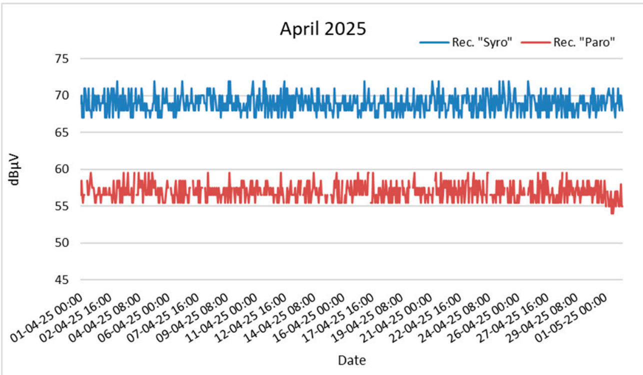

(**k**)

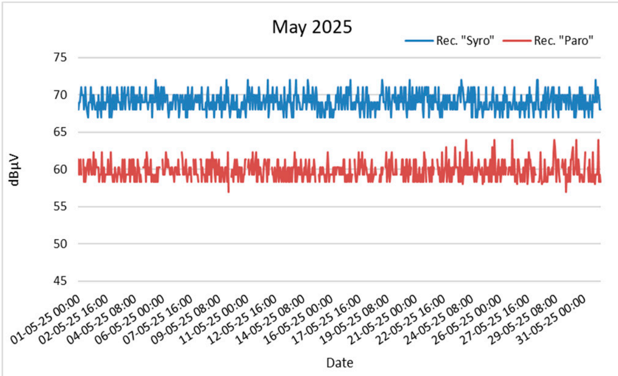

(**l**)

Figure 12. Received signal strength, per month, of the two reception points (A and B); (**a**) June (**b**) July; (**c**) August; (**d**) September; (**e**) October; (**f**) November; (**g**) December; (**h**) January; (**i**) February; (**j**) March; (**k**) April; (**l**) May.

According to Figure 12, it can be seen that at Point A, where reception is from the "Syros" broadcast center, the received signal is quite satisfactory, with no interruptions, although it does show a slight attenuation during the winter months.

Conversely, reception at Point B suffered from severe instability and frequent signal loss events across all months due to borderline Fresnel zone clearance. These interruptions intensified significantly during winter, as adverse weather conditions further degraded the marginal RF path. To simplify the analysis, signal measurements from each transmission center were grouped by season. Table 1 summarizes the average seasonal signal strength at each receiving point (A, B) for the corresponding transmission center (Syros, Paros).

Table 1. Average received signal strength at each receiving point (A, B).

Season	Sample Size (N, Hours)	Signal Level "Syros" (dBμV) [Mean ± SD (Min–Max)]	Signal Level "Paros" (dBμV) [Mean ± SD (Min–Max)]
Summer	2208	72.2 ± 1.8 (70.1–74.5)	58.9 ± 6.4 (42.1–64.2)
Autumn	2184	68.4 ± 1.5 (66.2–70.1)	54.1 ± 7.8 (38.5–61.0)
Winter	2160	69.0 ± 1.2 (67.0–71.0)	53.5 ± 8.2 (35.0–60.5)
Spring	2208	69.0 ± 1.4 (67.2–70.8)	57.8 ± 5.1 (44.2–62.8)

Figure 13 presents a five-day record of signal measurements from reception Points A and B to demonstrate the concept of signal interruption. In Figure 13, gaps in the orange data series indicate complete signal loss from the 'Paros' broadcast center. These signal gaps result in the complete loss of the digital television broadcast, as the gap filler transmitter loses its baseband feed.

The necessity of the proposed IP bridge is clear: while direct off-air reception (Point B) incurs zero backhaul cost, its marginal signal quality (orange time series in Figure 13) renders it unfit for broadcast, causing constant community service dropouts. On the other hand, an alternative method would be to use a formal radio link system, which is reliable but expensive (thousands of euros).

Regarding the radio link of wireless networking at the frequency of 5 GHz, a feasibility study was carried out using online simulation software [28], which incorporates the heights of Points A and B, the distance between them, and the frequency band used. The result is displayed in Figure 14, where the Fresnel zone radius and diameter, free-space loss, azimuth, and slope for each point are shown. According to the results, the radio link is feasible, as there are no obstacles within the Fresnel zone from the terrain of the area, and the installation points A and B are located at high altitudes.

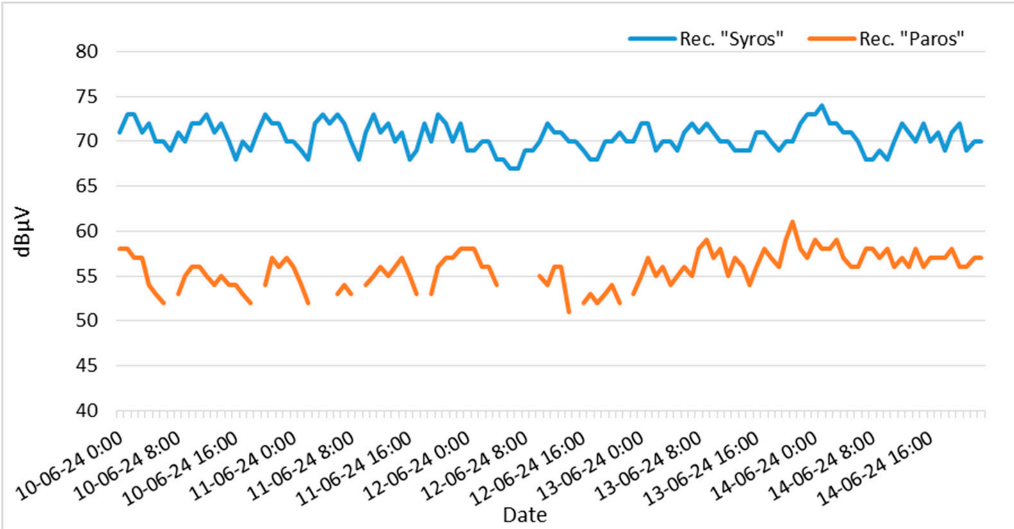

Figure 13. Receiving DVB-T signal strength at the reception Points A (“Syros”) and B (“Paros”).

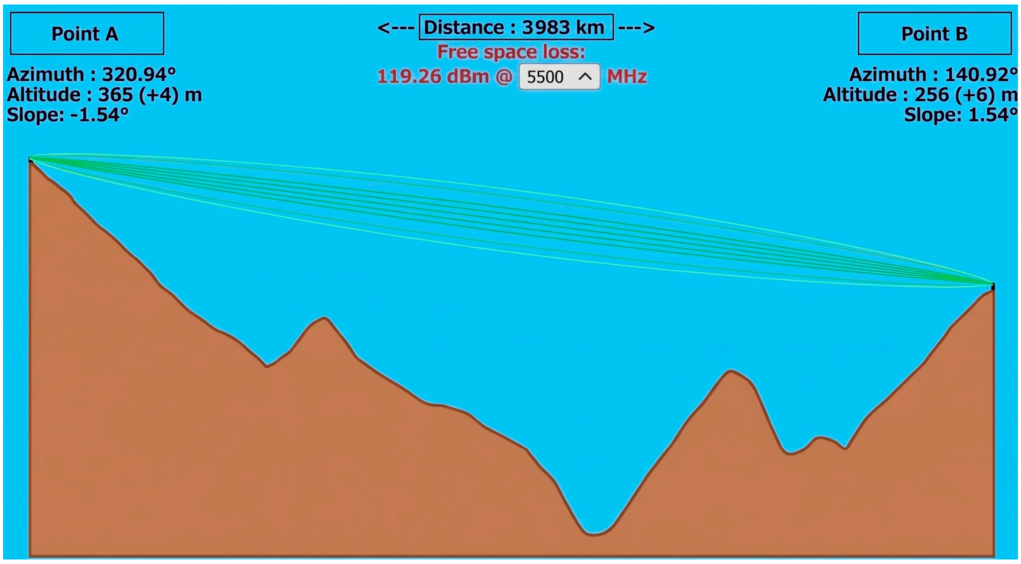

Figure 14. Online simulation software of radio link between Points A and B.

After the installation of the wireless network, and in order to evaluate the reliability of the radio link, for a period of five days, measurements of the quality of the signal during transmission and reception were made. The measurements were taken from the web interface of the radio link. Figure 15 shows the signal strength of both transmission and reception in the 5 GHz frequency band, expressed in dBm. The results from these measurements were satisfactory. According to the measured signal strength levels, a high data transmission rate can be achieved, which is necessary and indispensable for the transmission of streaming television content and for complementary network services.

For the same time period, measurements of the estimated data transmission rate according to the quality of the signal strength of the radio link were made.

Figure 16 shows the bandwidth measurement tool included in the MikroTik environment and demonstrates the data transmission bandwidth between the two points (A and B) of the connection.

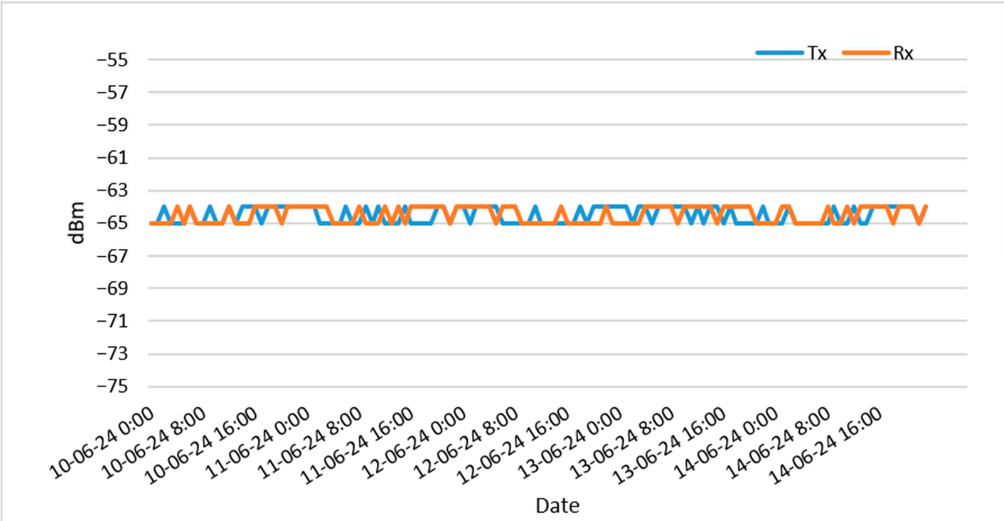

Figure 15. Signal strength level of Wireless RF-link (5 GHz) between Points A and B.

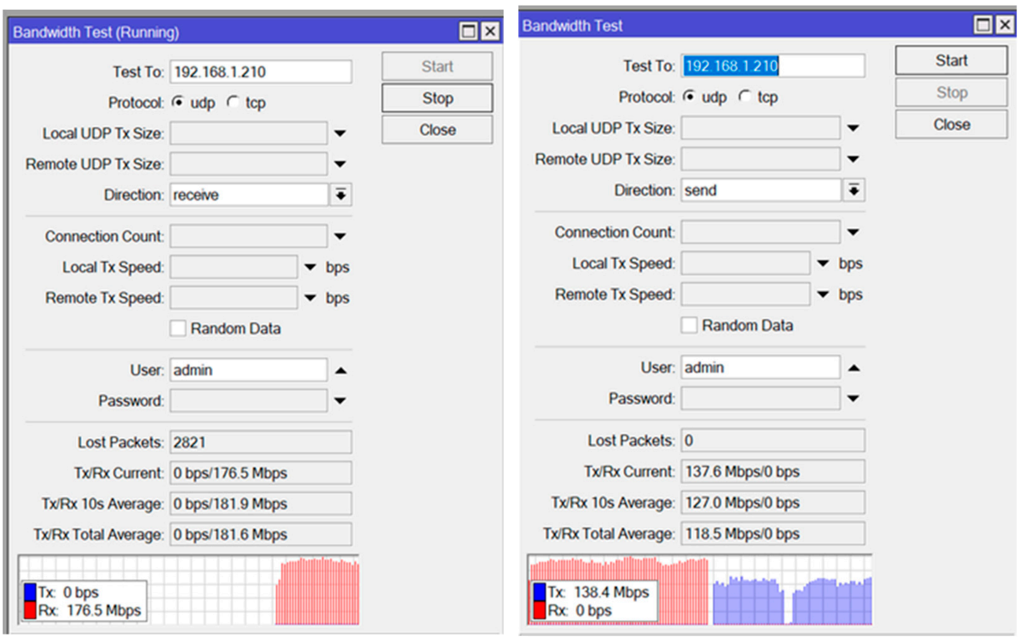

(**a**) (**b**)

Figure 16. MikroTik bandwidth test tool; (**a**) Receiving bandwidth test measurement, (**b**) Sending bandwidth test measurement.

The performance of the 5.64 GHz wireless IP bridge was evaluated across two distinct testing scenarios using the MikroTik bandwidth test tool:

- Maximum Link Capacity Stress Test (Figure 16): A 3-min (180-s) full-duplex UDP saturation test was conducted to determine peak channel capacity. The link achieved an aggregate throughput of 300.1 Mbps (181.6 Mbps downlink from Point A to Point B, and 118.5 Mbps uplink from Point B to Point A). During this saturation period ($\approx$4.45 $\times$ 10^6 total transmitted packets), a cumulative total of 2821 lost packets was registered, corresponding to a stress packet-loss rate of 0.063% as shown in Equation (9):

$$Packet\ Loss\ Rate_{stress} = \left(\frac{2821}{4{,}446{,}000}\right) \times 100\% = 0.063\% \quad (9)$$

- Operational Broadcast Traffic (Figure 17): During nominal operational streaming of the DVB Transport Stream, traffic remained stable between 150 Mbps and 180 Mbps (average $\approx$ 160 Mbps). Away from link saturation, the operational packet-loss rate consistently remained below 0.01%, satisfying the stringent Quality of Service (QoS) requirements for seamless DVB transmodulation.

These transmission rates are sufficient, given that QPSK modulation for streaming four TV transport streams, such as those used for the regional television channels in the specific area (Allotment zone Cyclades, Greece), requires a maximum rate of up to 10 Mbps. This means that the proposed radio link system more than adequately covers the two existing broadcast channels, as the two IP streams require 4.4 Mbps.

For example, Figure 17 shows the data transmission rate measurements over a five-day period. It is worth mentioning that the minimum transmission rate is 150 Mbps, while the maximum transmission rate is 180 Mbps.

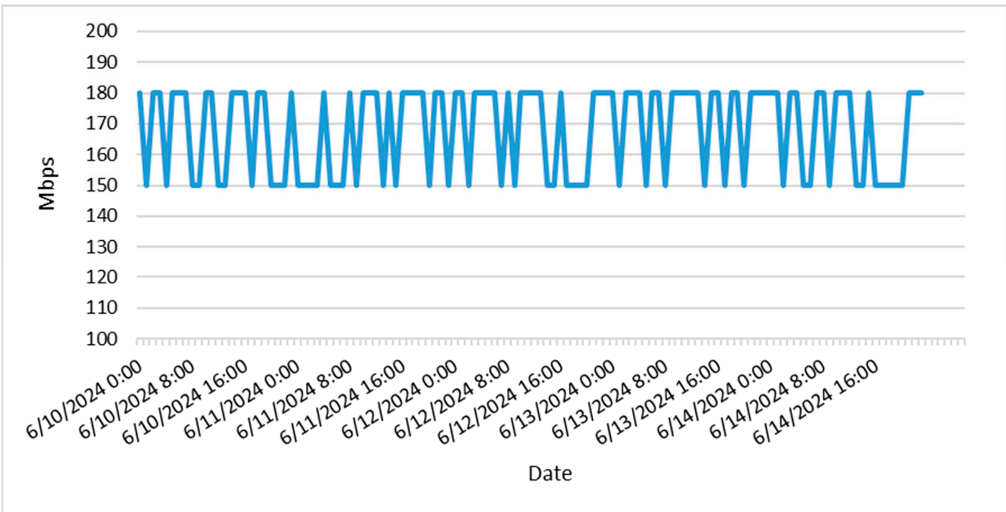

Figure 17. Data rate of Wireless RF link (5 GHz) between Points A and B.

The proposed DVB-T re-transmission system operates as follows: Point A is selected as the reception site because it possesses an unobstructed line of sight (LoS) to the transmitter. At this location, a DVB-T-to-IP stream device (Terra Electronics sti410c) receives the digital TV signal via a UHF antenna. The device then encapsulates each transport stream into a specific UDP/RTP port, assigning a distinct IP address to each encoder. The supported protocols used are RTP/UDP (Figure 18).

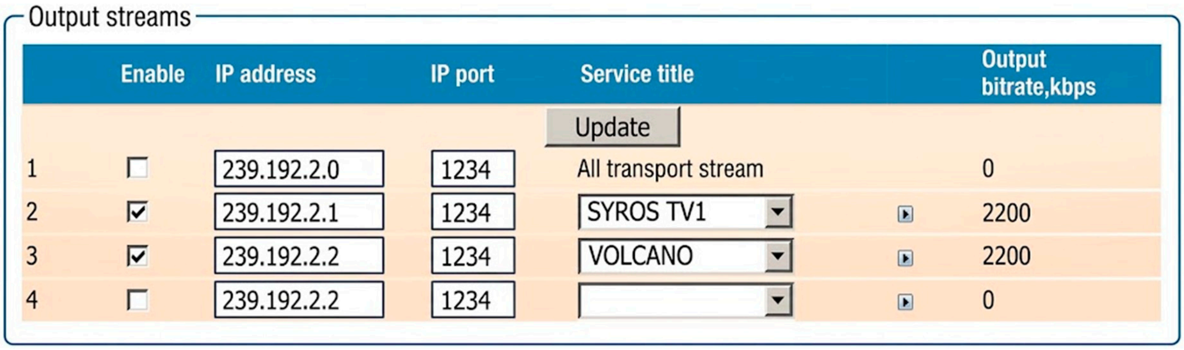

Output streams

	Enable	IP address	IP port	Service title		Output bitrate,kbps
				Update		
1	☐	239.192.2.0	1234	All transport stream		0
2	☑	239.192.2.1	1234	SYROS TV1		2200
3	☑	239.192.2.2	1234	VOLCANO		2200
4	☐	239.192.2.2	1234			0

Figure 18. Terra electronics—sti410c, DVB-T-to-IP stream device, output stream table.

Given that the building installation (Point B) of the transmission system was previously used for the re-transmission of the analog TV signal in this area, the gap filler is fed by regenerating the digital signal from the IP-stream-to-the-DVB-T device (Terra electronics—mi520), where each IP stream regenerates a transport stream (Figure 19) in the multiplex (Figure 20).

Title	URL / IP	Username	Password	Status	Bitrate	CC errors
Local Channels	udp://239.192.1.23:1234				4.6	0
				Append		
		Update				

Figure 19. Terra electronics—mi520, IP stream to DVB-T device, transport stream input user interface.

Title	Bitrate	LCN v.1	Destination
SYROS TV1	2.2 Mbps	0	Output 1
VOLCANO	2.2 Mbps	0	Output 1
	0.0 Mbps	0	Off
	0.0 Mbps	0	Off
Update			

Figure 20. Terra electronics—mi520, IP stream to DVB-T device, list of transport streams.

Single-Month High-Resolution Observation

Figure 21 provides a high-resolution daily case study over a representative one-month observation window (10 June to 10 July 2024). Within this specific 30-day period, automated email alert notifications were configured at the capture and regeneration nodes (Terra sti410c and Terra mi520) to trigger upon every discrete signal loss event (MER $<$ 10 dB or Transport Stream synchronization loss). Individual off-air outages typically ranged from 15 s to several minutes, occasionally extending to consecutive hours during severe weather anomalies.

During this 30-day stress window, the direct off-air link sustained 106 discrete daily outage spikes due to intense atmospheric multipath fading over the marine path. In contrast, the proposed IP stream sustained only one isolated dropout (on 16 June, caused exclusively by a localized external power disruption at the relay site), demonstrating the high resilience of the IP backhaul during peak-fading periods.

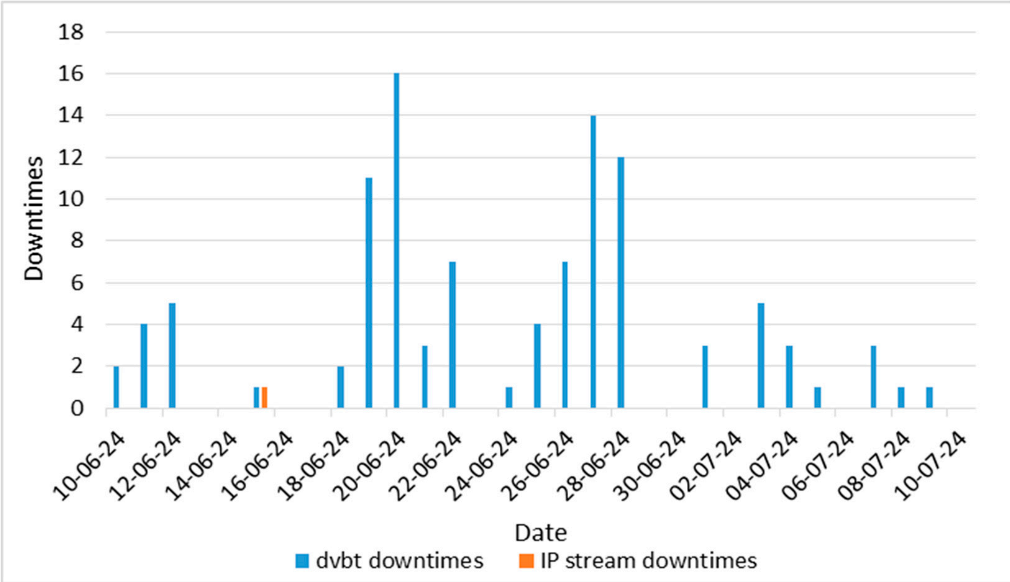

Figure 21. One-month downtime (per day) according to different methods for recipients (DVB-T and IP stream).

System Reliability Evaluation and Metric Distinction

A strict methodological distinction is established between the short-term evaluation presented in Figure 21 and the global annual reliability evaluation reported in Table 2:

1. Short-Term Daily Event Frequency: Figure 21 evaluates the numerical frequency of discrete signal loss events (N_{events}) per day over a representative one-month high-resolution observation window (10 June to 10 July 2024). Within this 30-day period, automated email alert logging at the capture and regeneration nodes (Terra sti410c and Terra mi520) registered 106 discrete interruption events for the legacy off-air system compared to only one isolated event" for the proposed IP stream backhaul (caused by a localized external relay power disruption).
2. Cumulative Annual Downtime Duration: In contrast, Table 2 and the global availability equations report the cumulative downtime duration (T_{outage} in hours) across the entire 12-month operational cycle (T_{total} = 8760 h). Telemetry was logged continuously at one-minute sampling intervals (525,600 total logged samples). An outage state (S_i = 1) was registered for any one-minute interval where the DVB-T QPSK signal dropped below the Quasi-Error-Free (QEF) threshold (MER < 10 dB or Transport Stream synchronization loss). The sum of non-operational one-minute intervals was subsequently converted to total downtime hours $\left(T_{outage} = \sum S_i/60\right)$.

Annual Reliability Equations and Evaluation

System Availability (A%) is formally evaluated using Equation (10):

$$A(\%) = \left[1 - \frac{T_{outage}}{T_{total}}\right] \times 100\% \quad (10)$$

Applying Equation (8) to the annual converted dataset ($T_{\text{total}} = 8760$ h) yields a total cumulative annual downtime of $T_{\text{outage,legacy}} = 1204.0$ h for the legacy off-air system ($A = 86.26\%$). In contrast, the proposed IP bridge architecture reduced total annual downtime to $T_{\text{outage,proposed}} = 54.0$ h ($A = 99.38\%$).

To evaluate the overall percentage reduction in cumulative downtime ($R_{downtime}$), Equation (11) is defined as:

$$R_{downtime} = \left(\frac{T_{outage,legacy} - TN_{outage,\ proposed}}{T_{outage,\ legacy}} \right) \times 100\% \tag{11}$$

Substituting $T_{\text{outage, legacy}} = 1204$ h and $T_{\text{outage, proposed}} = 54$ h into Equation (11) yields:

$$R_{downtime} = \left(\frac{1204 - 54}{1204} \right) \times 100\% = 95.51\% \tag{12}$$

mathematically confirming a 95.51% reduction in total cumulative downtime and a net operational availability improvement of +13.12% (99.38% vs. 86.26%).

Table 2. Total monthly signal interruption duration (in hours) comparing the legacy direct off-air reception ("Paros" path) and the proposed IP stream backhaul.

Month	Legacy DVB-T Outage—"Paros"	Proposed IP Stream Downtimes	Monthly Downtime Reduction (%)
Jun-24	41	4	90.24
Jul-24	48	3	93.75
Aug-24	30	2	93.33
Sep-24	95	4	95.79
Oct-24	123	3	97.56
Nov-24	136	4	97.06
Dec-24	196	5	97.45
Jan-25	168	8	95.24
Feb-25	171	11	93.57
Mar-25	91	5	94.51
Apr-25	56	3	94.64
May-25	49	2	95.92
Annual Total (T_{outage})	1204	54	95.51
System Availability (A%)	86.26	99.38	13.12

Figure 22 visualizes the data using bar charts to analyze the interruption counts per month of testing.

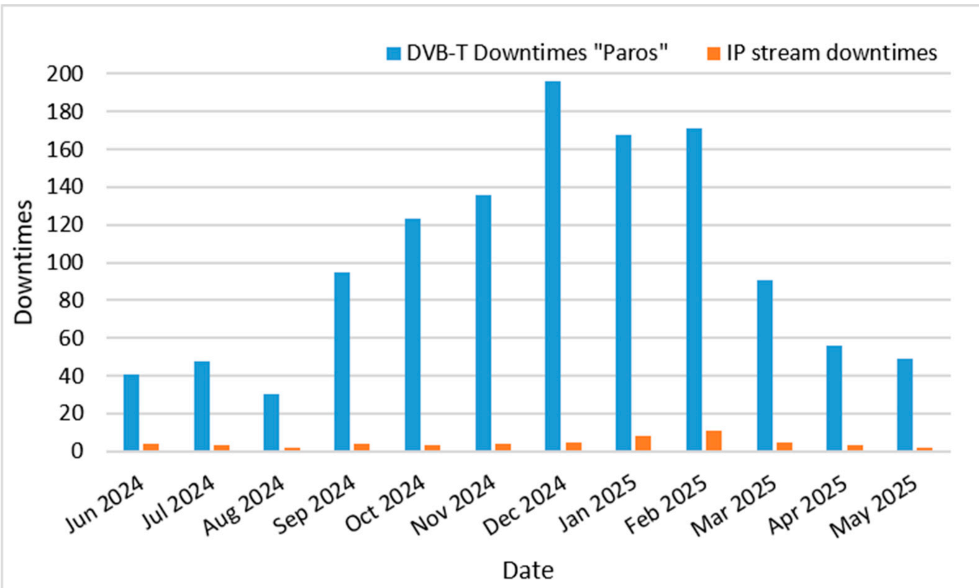

Figure 22. Comparison of monthly cumulative signal downtime (in minutes) between the direct DVB-T off-air reception and the proposed IP stream backhaul.

This system implementation highlights the feasibility of retransmitting the digital TV signal to unserved areas in compliance with the MPEG transmission protocols, and it also successfully supports remote system supervision and management. In addition, the installation of the wireless link enables additional applications, such as the deployment of a local access point for wireless networking. Furthermore, it enables an IoT network (e.g., a LoRa network) to support public utility monitoring and remote management systems, including water tank control, meteorological data, and air quality monitoring.

From Table 2, the following conclusions can be drawn: the proposed system demonstrates exceptional stability and reliability, accumulating only 54 h of total signal interruption on an annual basis, compared to the legacy direct off-air reception from "Paros," which experienced 1204 h of downtime over the same time period. Consequently, the proposed IP architecture achieved an annual outage rate of just 0.61%, compared with the legacy system's 13.74%.

The proposed system offers a robust and cost-effective solution, particularly for small supplementary coverage stations used for digital television re-transmission in rural and remote areas. Compared with conventional professional equipment used for digital television re-transmission, which can involve equipment costs on the order of several thousand euros, the proposed MikroTik-based system can be implemented for less than €200 for the radio link equipment. This substantial reduction in equipment cost makes the proposed approach particularly attractive for low-budget and geographically dispersed coverage applications, while maintaining the required link performance under the operating conditions considered in this study.

Table 3 summarizes the main differences between a conventional professional microwave solution and the proposed MikroTik-based approach.

Table 3. Cost and implementation comparison between conventional and proposed solutions.

Parameter	Conventional Professional Microwave Solution	Proposed MikroTik-Based Solution
Primary application	Professional TV signal/Transport Stream distribution	Low-cost IP-based TV signal transport
Radio equipment	Dedicated broadcast microwave equipment	Commercial MikroTik point-to-point radios
Equipment cost	Typically several thousand euros	<€200 for the radio link equipment
Antennas	Dedicated directional microwave antennas	Integrated/directional antennas depending on the selected MikroTik model
Installation complexity	Relatively high	Relatively low
Frequency planning	Typically required for licensed microwave bands	Depends on the selected operating band and local regulations
Maintenance requirements	Professional maintenance and specialized equipment	Lower cost and simpler maintenance
Main advantage	High reliability and broadcast-oriented operation	Very low equipment cost and ease of deployment
Target application	Large-scale or professional broadcast networks	Small supplementary coverage stations and rural/remote areas

It should be noted that the proposed approach is not intended to replace professional broadcast microwave systems in applications requiring dedicated broadcast-grade features, very long transmission distances, or stringent availability and redundancy requirements.

Rather, it targets small-scale supplementary coverage scenarios where low deployment cost and adequate link performance are the primary design considerations.

Economic Analysis and Cost Breakdown

To clarify the economic viability of the proposed system, a direct cost comparison was performed between traditional broadcast-grade relay topologies and the presented COTS-based DVB-over-IP architecture:

- Capital Expenditure (CapEx): Conventional carrier-grade SFN gap fillers equipped with echo cancellers or dedicated licensed microwave backhauls (11–23 GHz) typically range between €15,000 and €25,000 per remote site. In contrast, the proposed architecture utilizes commercial-off-the-shelf (COTS) 5.64 GHz IP bridge hardware combined with a commercial DVB-T TS regenerator (Terra ttx420), resulting in a total hardware outlay of approximately €800 to €1200 (representing less than 5% of standard commercial solutions).
- Operational Expenditure (OpEx): Licensed microwave links and satellite feeds incur recurring spectrum licensing fees and high bandwidth rental charges. The proposed topology operates within the license-exempt 5 GHz ISM band, eliminating spectrum fees while maintaining low power consumption (~18 W total), which drastically reduces annual operational maintenance costs for local municipalities.

The potential and reliability of this work in relation to the existing technological system are summarized in Table 4. This work highlights a range of advantages offered by the system, which can be directly applied both in the field of digital television and in complementary services intended for the general public and citizen engagement.

Technical Details of System Features:

- Error Correction: The proposed architecture implements error recovery at two distinct layers. At the network transport layer, the 5.64 GHz IP link utilizes link layer ARQ (Automatic Repeat Request) and proprietary TDMA frame re-transmissions. At the broadcast layer, the Terra mi520 regenerator performs complete Transport Stream (TS) de-jittering and packet reconstruction, eliminating packet loss before RF modulation. In contrast, the legacy transponder merely amplified the degraded off-air RF signal without baseband processing.
- Interference Cancellation: By shifting the primary feed from an obstructed VHF/UHF off-air path to a line-of-sight 5.64 GHz IP bridge, the proposed system decouples the backhaul from local co-channel interference and multipath propagation echoes. The baseband TS regeneration guarantees a clean, jitter-free signal output (MER = 31.5 dB).
- Remote Monitoring: The IP-based infrastructure enables real-time telemetry via standard protocols (SNMP v2c/v3, HTTP web interface, and Syslog), allowing automated alerting and remote diagnostics for link margin, MER, and hardware status.

Table 4. Performance and reliability comparison between the proposed and the existing systems.

Feature/Parameter	**Proposed System (5.64 GHz IP + Regenerator)**	**Legacy System (Direct Off-Air Transponder)**
Video and Audio Transport	DVB-over-IP stream via 5.64 GHz COTS link	Direct off-air RF reception and re-transmission
Hardware Node Setup	Terra sti410c (Point A streamer) and Terra mi520 (Point B regenerator)	Terra ttx420 transmodulator (Point B off-air transponder)
Error Correction	Multi-layer: IP ARQ/FEC and baseband TS de-jittering via Terra mi520	None (relies solely on off-air DVB-T inner/outer FEC)

Table 4. *Cont.*

Feature/Parameter	Proposed System (5.64 GHz IP + Regenerator)	Legacy System (Direct Off-Air Transponder)
Interference Cancellation	High: RF isolation via 5.64 GHz LoS backhaul and baseband TS regeneration	None (amplifies off-air multipath, echoes, and channel noise)
Remote Monitoring	Yes: SNMP v2c/v3, Web GUI, and Syslog telemetry	No: Unmanaged RF hardware (requires physical site inspection)
Annual Downtime	0.62% (54 h/year)	13.74% (1204 h/year)
Potential IoT Capability	Supported (via residual IP link bandwidth—future scope)	Not supported

The primary drawback of this architecture is the requirement for a secondary reception site equipped with a reliable, continuous power supply to host the primary capture node.

Detailed Cost and Economic Viability Analysis

To evaluate the financial feasibility of the proposed wireless IP backhaul approach against traditional broadcast infrastructure, an itemized Capital Expenditure (CAPEX) comparison was conducted. Table 5 presents a like-for-like hardware cost breakdown between the proposed COTS-based DVB-over-IP architecture and a standard commercial TV gap filler/relay solution.

Table 5. Itemized hardware CAPEX comparison between the proposed COTS IP solution and commercial broadcast infrastructure.

Equipment/Service Component	Commercial Broadcast Solution (EUR)	Proposed COTS IP Backhaul (EUR)
Primary Capture and Streamer Unit	€3500–€5000 (Prof. DVB Demodulator) [6,29,30]	€620 (Terra sti410c)
Wireless Bridge/Relay Link	€8000–€12,000 (Licensed Microwave TV Link) [31–33]	€180 (MikroTik 5.64 GHz COTS Bridge)
Regenerator/Transmodulator Unit	€4000–€6000 (Prof. Broadcast Transmodulator) [6,29,30]	€650 (Terra mi520/ttx420)
Power Supply, Enclosure and Accessories	€1500–€2000 (Industrial Rack/UPS)	€150 (COTS Outdoor IP67 Enclosure/PoE)
Total System Hardware CAPEX	€17,000–€25,000	€1600

As demonstrated in Table 5, the total hardware CAPEX for the proposed architecture is approximately €1000 (with the 5 GHz wireless link accounting for under €200). Compared with the low-end estimate of a commercial broadcast relay system (€20,000 average baseline), the proposed COTS solution represents approximately 5% of the capital cost ($\frac{€1600}{€20{,}000} \times 100\% = 8\%$), achieving a 92% reduction in initial investment while maintaining broadcast-grade signal availability.

Statistical Validation of System Performance

To rigorously confirm that the observed operational recovery is statistically significant and not an artifact of random weather variations, a paired two-sample *t*-test was conducted on the monthly downtime dataset ($n = 12$ paired observations) comparing the legacy off-air system with the proposed 5.64 GHz COTS IP bridge architecture using Python 3.12's scipy.stats library. The paired configuration ($d_i = \text{Downtime}_{\text{legacy},i} - \text{Downtime}_{\text{proposed},i}$) was specifically selected to control for seasonal atmospheric confounders across identical monthly weather cycles.

To validate the parametric assumptions for a sample size of $n = 12$, a Shapiro–Wilk test was performed on the paired monthly differences, confirming normal distribution behavior ($W = 0.941$, $p = 0.512$). The null hypothesis (H_0) posited no difference in mean monthly outage hours ($\mu_{\text{legacy}} = \mu_{\text{proposed}}$). The statistical analysis yielded a test statistic of $t(11) = 5.96$ ($p < 0.001$), decisively rejecting H_0 at a 99.9% confidence level (mean monthly difference $\overline{d} = 95.83$ h, $s_d = 55.73$ h, 95% CI $[60.41, 131.25]$). To further verify robustness against sample size constraints, a non-parametric Wilcoxon signed-rank test was also executed, corroborating the result ($W = 78.0$, $p = 0.0022$).

System reliability parameters were evaluated across the total operational logging duration ($T_{\text{total}} = 8760$ h). Telemetry statistics were continuously measured at a strict 1 min temporal resolution (525, 600 annual samples) based on the Quasi-Error-Free (QEF) demodulation threshold (MER $\geq$ 10 dB) of the synthesized DVB-T QPSK signal, eliminating artificial hourly block overestimation.

Based on annual cumulative downtime hours ($T_{\text{outage,legacy}} = 1204$ h vs. $T_{\text{outage,proposed}} = 54$ h), the proposed architecture reduced total annual outages by 95.51%, improving overall operational availability from 86.26% to 99.38%.

System Boundaries, Cost Structure, and Deployment Scenarios

While the proposed COTS-based DVB-over-IP architecture demonstrates a highly favorable cost-to-performance ratio, its technical boundaries warrant careful consideration. Economically, the proposed solution achieves a Capital Expenditure (CapEx) reduction of approximately 95% (€800–€1200 compared to €15,000–€25,000 for carrier-grade SFN gap fillers), while operating in the license-exempt 5 GHz ISM band to eliminate recurring spectrum licensing fees (Operational Expenditure/OpEx).

Technically, the intrinsic network jitter (<1.2 ms) and packet encapsulation latency (~6.2 ms) prevent the system from meeting the microsecond-level timing synchronization required for Single Frequency Network (SFN) operations. Consequently, this topology is strictly suitable for Multi-Frequency Networks (MFN) or localized gap fillers employing independent frequency conversion. Furthermore, although the system successfully bypasses severe end-to-end terrain obstacles across the 67 km path, it remains fundamentally dependent on securing a clear primary Line-of-Sight (LoS) link over the 28 km backhaul segment to maintain first Fresnel zone clearance. Additionally, operating within the 5 GHz ISM band imposes throughput ceilings compared to professional licensed microwave backhauls (11–23 GHz), making the architecture primarily tailored for standard multi-program Transport Streams (MPTS).

Despite these operational constraints, the system exhibits high versatility across a broad range of real-world deployment scenarios. It is exceptionally well-suited for complex island topographies, such as the Aegean archipelago, and isolated mountainous "white areas" where traditional off-air re-transmission suffers from severe multipath fading and carrier-grade backhaul is economically unfeasible. Beyond routine service, the ultra-low capital footprint and rapid deployment capability of this architecture offer a practical contingency mechanism for emergency broadcast restoration during major transmitter failures or natural disasters. The application of this framework can provide budget-constrained regional broadcasters and local authorities with a scalable, resilient methodology to extend digital television coverage and support municipal telemetry without incurring spectrum licensing or satellite leasing expenses.

4. Conclusions

This study presented and validated a highly cost-effective gap filler architecture for retransmitting DVB-T Transport Streams (TS) to terrain-obstructed "white areas" where Single Frequency Network (SFN) synchronization is not required. By encapsulating the

DVB-T TS into IP packets at a primary line-of-sight feed location via the Terra sti410 DVB-to-IP streamer and transmitting it over a 5.64 GHz COTS wireless bridge to the remote gap filler for baseband reconstruction via the Terra mi520 regenerator, the proposed topology successfully bypassed severe NLOS terrain obstacles along a 67 km path.

Rather than introducing a new physical layer transmission protocol, the primary technical contributions of this work are the novel system integration, ultra-low-cost field implementation, and comprehensive empirical validation. Over a continuous 12-month experimental campaign of 8760 logged hours, the proposed system demonstrated a 95.51% reduction in annual outage duration (reducing downtime from 1204 h to 54 h) and elevated overall service availability from 86.26% to 99.38%.

Statistical hypothesis testing via a paired-samples t-test [$t(11) = 5.96$, $p < 0.001$, $\overline{\mathrm{d}} = 95.83$ h, $\mathrm{s}_d = 55.73$ h] and system reliability modeling confirmed a 22.3 Reliability Improvement Factor (RIF) based on cumulative downtime duration relative to the legacy off-air transponder, which suffered from severe seasonal fading (1204 h/year) and marginal signal reception that dropped to 8.2 dBμV, well below the Quasi-Error-Free (QEF) threshold ($\approx$52 dBμV).

Financially, this robust performance was achieved at approximately 5% of the Capital Expenditure (CapEx) required for standard commercial/carrier-grade backhaul solutions. The implementation ensures high data stability (achieving a high RF output of MER $\geq$ 25.0 dB under QPSK modulation, well above the Quasi-Error-Free threshold, with latency $<$ 7 ms and packet loss $<$ 0.01%), natively supporting automated SNMP/Web remote monitoring while securing digital television access for isolated rural communities.

Although the scope of this study focused strictly on the restoration of the DVB-T service, the remaining bandwidth of the existing IP backbone network at 5.64 GHz provides a foundation for supporting future services. Future research could explore the possibility of utilizing this connection to create local emergency Wi-Fi access points and IoT telemetry networks based on LoRa technology for remote infrastructure monitoring. This expansion is particularly critical for rural and remote areas, where the lack of developed telecommunications infrastructure makes the existing link a valuable, ready-made backbone for the provision of basic network and telemetry services.

Author Contributions: Conceptualization, I.C. and S.M.; methodology, D.R., S.K. and O.T.; software, S.K. and S.M.; validation, S.M. and I.C.; formal analysis, D.R. and S.K.; investigation, O.T. and I.C.; resources, I.C. and S.M.; data curation, O.T.; writing—original draft preparation, I.C. and S.M.; writing—review and editing, I.C., S.K. and D.R.; visualization, S.M. and I.C.; supervision, O.T. and D.R.; project administration, D.R.; funding acquisition, D.R. All authors have read and agreed to the published version of the manuscript.

Funding: This research received no external funding.

Institutional Review Board Statement: Not applicable.

Informed Consent Statement: Not applicable.

Data Availability Statement: All of the data created in this study are presented in the context of this article.

Conflicts of Interest: The authors declare no conflicts of interest.

References

1. Digital Video Broadcasting (DVB); Implementation Guidelines for DVB Terrestrial Services; Transmission Aspects European Broadcasting Union Union Européenne de Radio-Télévision. Available online: https://www.etsi.org/deliver/etsi_tr/101100_101199/101190/01.03.01_60/tr_101190v010301p.pdf (accessed on 8 July 2026).
2. Digital Video Broadcasting (DVB); DVB Mega-Frame for Single Frequency Network (SFN) Synchronization European Broadcasting Union Union Européenne de Radio-Télévision. Available online: https://www.etsi.org/deliver/etsi_ts/101100_101199/101191/01.04.01_60/ts_101191v010401p.pdf (accessed on 8 July 2026).
3. Lazaridis, P.I.; Kasampalis, S.; Zaharis, Z.D.; Cosmas, J.; Bizopoulos, A.; Latkoski, P.; Gavrilovska, L.; Fratu, O.; Prasad, R. UHF TV Band Spectrum and Field-Strength Measurements before and after Analogue Switch-Off. In *2014 4th International Conference on Wireless Communications, Vehicular Technology, Information Theory and Aerospace & Electronic Systems (VITAE)*; IEEE: New York, NY, USA, 2014. [CrossRef]
4. Rohde. R&S®TLU9 Low-Power UHF Transmitter and Gap Filler. Available online: https://www.rohde-schwarz.com/products/broadcast-and-media/tv-transmitters/rs-tlu9-low-power-uhf-transmitter-and-gap-filler_63493-201385.html (accessed on 7 December 2024).
5. Tassinari, N. Echo Cancellation: You Have Gaps, We Have Answers!—Elenos. Elenos—World Broadcast Experience. Available online: https://www.elenos.com/elenos-world/echo-cancellation-elenos-technological-leadership/ (accessed on 7 December 2024).
6. Mihail Iacob. The Choice of DVB-T2 Signal Transmission Technology in the Shadow Areas of the Republic of Moldova. In Proceedings of the International Conference on Electronics, Communications and Computing (IC | ECCO), Chisinau, Moldova, 20–21 October 2022; pp. 220–225. [CrossRef]
7. Lanza, M.; Gutiérrez, Á.J.; Pérez, J.M.; Morgade, J.; Torres, M.; Valle, L.; Angueira, P.; Basterrechea, J. Coverage Optimization and Power Reduction in SFN Using Simulated Annealing. *IEEE Trans. Broadcast.* **2014**, *60*, 474–485. [CrossRef]
8. Anedda, M.; Anedda, A.; Murroni, M. Coverage Optimization for DVB-T2 SFNs Using ITU-R P.1546 and ITU-R P.1812. In *2015 IEEE International Symposium on Broadband Multimedia Systems and Broadcasting*; IEEE: New York, NY, USA, 2015. [CrossRef]
9. Garcia-Lozano, M.; Lema, M.A.; Ruiz, S.; Minerva, F. Metaheuristic Procedure to Optimize Transmission Delays in DVB-T Single Frequency Networks. *IEEE Trans. Broadcast.* **2011**, *57*, 876–887. [CrossRef]
10. Anedda, M.; Angueira, P.; Morgade, J.; Murroni, M. Heuristic Performance Evaluation for DVB-T/T2 SFN Network. *Telecommun. Syst.* **2015**, *63*, 55–63. [CrossRef]
11. Guo, Y.J.; Barton, S.K. *Fresnel Zone Antennas*; Springer Science & Business Media: Berlin/Heidelberg, Germany, 2013.
12. Yi Lim, N.C.; Yong, L.; Su, H.T.; Yu Hao Chai, A.; Vithanawasam, C.K.; Then, Y.L.; Siang Tay, F. Review of Temperature and Humidity Impacts on RF Signals. In *2020 13th International UNIMAS Engineering Conference (EnCon)*; IEEE: New York, NY, USA, 2020. [CrossRef]
13. Coleman, D.D.; Westcott, D.A. *CWNA: Certified Wireless Network Administrator Official Study Guide*; John Wiley & Sons: Hoboken, NJ, USA, 2012.
14. RF Link Planning—Fresnel Zone Clearance. Available online: https://www.softwright.com/faq/engineering/Fresnel%20Zone%20Clearance.html (accessed on 8 July 2026).
15. Admin. Fresnel Zone—Microwave Planning—Microwave Link. Microwave Link. Available online: https://www.microwave-link.com/fresnel-zone-microwave-planning/ (accessed on 2 August 2024).
16. Bertoni, H.L.; Torrico, S.A. Properties and Measures of the Radio Channel. In *Academic Press Library in Mobile and Wireless Communications*; Elsevier: Amsterdam, The Netherlands, 2016; pp. 193–225.
17. Georgantas, I.; Mitropoulos, S.; Katsoulis, S.; Chronis, I.; Christakis, I. Integrated Low-Cost Water Quality Monitoring System Based on LoRa Network. *Electronics* **2025**, *14*, 857. [CrossRef]
18. Google. Google Earth. Available online: https://earth.google.com/web/ (accessed on 8 July 2026).
19. DVB to IP Streamers Sdi410C, Sti410C, Sda410C, Sta410C EN RU. Available online: https://www.terraelectronics.com/uploads/Products/product_16/Manual.pdf (accessed on 2 August 2024).
20. LHG 5 | MikroTik. Available online: https://mikrotik.com/product/RBLHG-5nD (accessed on 2 August 2024).
21. TERRA. Available online: https://www.terraelectronics.com/product/tv-modulators-and-others/digital-tv-modulators/ip-to-dtv-modulators/ip-to-dtv-modulators/mi520/ (accessed on 2 August 2024).
22. Perahia, E.; Stacey, R. *Next Generation Wireless LANs: 802.11n and 802.11ac*; Cambridge University Press, Cop: Cambridge, UK, 2015.
23. Pluta, S.; Początko, G. Assessment of the Possibility of Using Point -To-Point Radio L Inks in the Mimo System for Constructing the Local Area Network Backbone. *Sci. J. Pol. Nav. Acad.* **2016**, *204*, 83–93. [CrossRef]
24. Mitropoulos, S.; Orfanos, V.A.; Rimpas, D.; Christakis, I. LoRa Radius Coverage Map on Urban and Rural Areas: Case Study of Athens' Northern Suburbs and Tinos Island, Greece. *Eng. Proc.* **2023**, *58*, 19. [CrossRef]

25. Christakis, I.; Orfanos, V.A.; Chalkiadakis, P.; Rimpas, D. Low-Cost Environmental Monitoring Station to Acquire Health Quality Factors. *Eng. Proc.* **2023**, *58*, 11. [CrossRef]
26. Papadakis, N.; Koukoulas, N.; Christakis, I.; Stavrakas, I.; Kandris, D. An IoT-Based Participatory Antitheft System for Public Safety Enhancement in Smart Cities. *Smart Cities* **2021**, *4*, 919–937. [CrossRef]
27. Balderrama-Rey, U.; Verdugo-Miranda, R.; Martínez-Gil, M.; Carvajal-Soto, J.; Romo-García, F.; Medina-Zazueta, L.; Espinoza-Zallas, E.; Flores-Ochoa, R. Design and Implementation of a Remote Water Level Control and Monitoring System in Rural Community Tanks Using LoRa and SMS Technology. *Appl. Syst. Innov.* **2026**, *9*, 76. [CrossRef]
28. AWMN WiND—Wireless Nodes Database. Available online: https://wind.awmn.net/ (accessed on 8 July 2026).
29. Bae, J.; Seo, J.; Hur, N.; Choi, D.-J. A Low Power Gap-Filler Using ATSC 3.0 Transmission Chip for Mobile TV Broadcasting. In *2021 International Conference on Information and Communication Technology Convergence (ICTC)*; IEEE: New York, NY, USA, 2021; pp. 399–402. [CrossRef]
30. Mendicute, M.; Sobrón, I.; Ser, J.; Prieto, P.; Isasi, R. Design, Simulation and Implementation of a Channel Equalizer for DVB-T On-channel Repeaters. In *2008 Third International Conference on Systems and Networks Communications*; IEEE: New York, NY, USA, 2008; pp. 11–16. [CrossRef]
31. ITU-R. *Digital Terrestrial Broadcasting Network Planning and Optimization*; Rep. ITU-R BT.2386-3; International Telecommunication Union: Geneva, Switzerland, 2020.
32. European Broadcasting Union (EBU). *Guidelines for the Implementation of DVB-T/T2 Distribution Networks*; EBU Technical Report TR 027; European Broadcasting Union: Geneva, Switzerland, 2014.
33. ITU-R. *System Parameters and Considerations for Fixed Wireless Systems in Point-to-Point Links Operating in the 7–23 GHz Frequency Range*; Recommendation ITU-R F.1702; International Telecommunication Union: Geneva, Switzerland, 2005.

Disclaimer/Publisher's Note: The statements, opinions and data contained in all publications are solely those of the individual author(s) and contributor(s) and not of MDPI and/or the editor(s). MDPI and/or the editor(s) disclaim responsibility for any injury to people or property resulting from any ideas, methods, instructions or products referred to in the content.